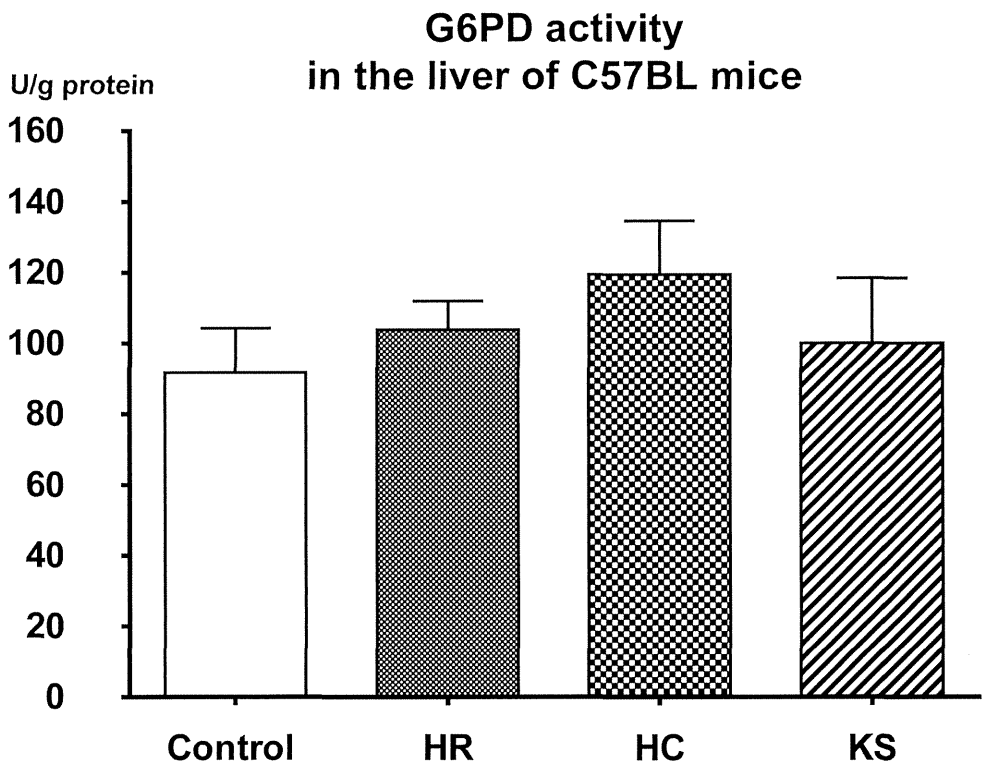

Figure 16　G6PD activity in the liver of C57BL mice

Male C57BL mice were fed on AIN-93G diet containing 7w/w% HR, HC or KS as the sole dietary fat for 30 weeks.　N=5.

HR, rapeseed oil containing　medium chain fatty acids of　coconut oil origin; HC, mixtureof rice-bran oil and canola oil; soybean oil added with phytosterols

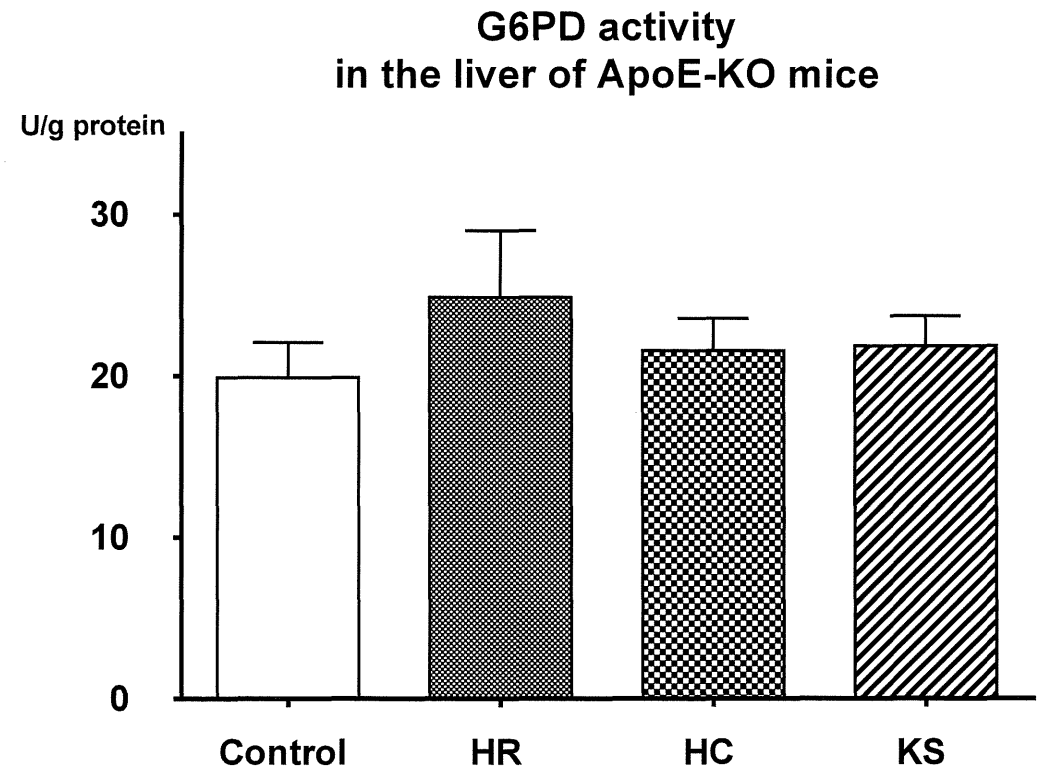

Figure 17 G6PD activity in the liver of ApoE-KO mice

Male ApoE-KO mice were fed on AIN-93G diet containing 7w/w% HR, HC or KS as the sole dietary fat for 30 weeks. N=4-5.

HR, rapeseed oil containing medium chain fatty acids of coconut oil origin; HC, mixtureof rice-bran oil and canola oil; soybean oil added with phytosterols

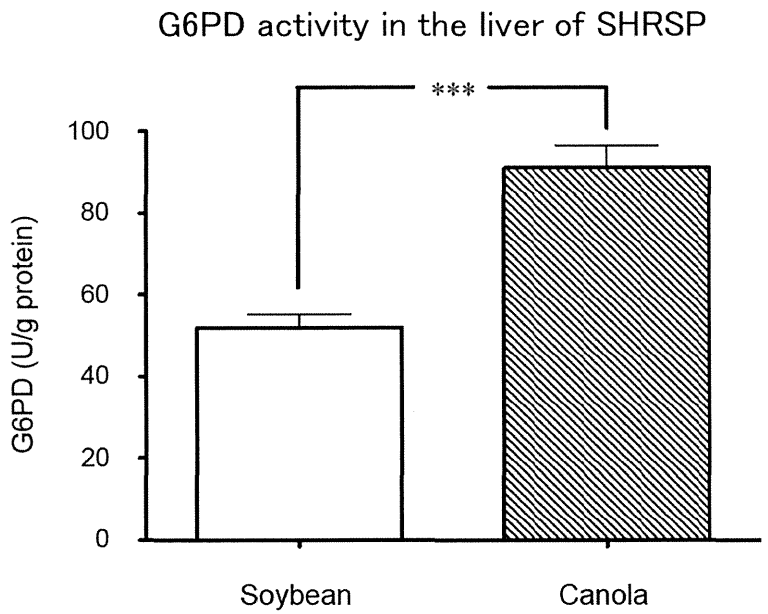

Figure 18　G6PD activity in the liver of SHRSP

Male SHRSP were fed on AIN-93G diet without fat and given soybean oil or canola oil by gavage for 8 weeks. The daily amount of each oil given corresponded with 10w/w% of daily food intake.　N=10.　***$p<0.001$ (unpaired t-test).

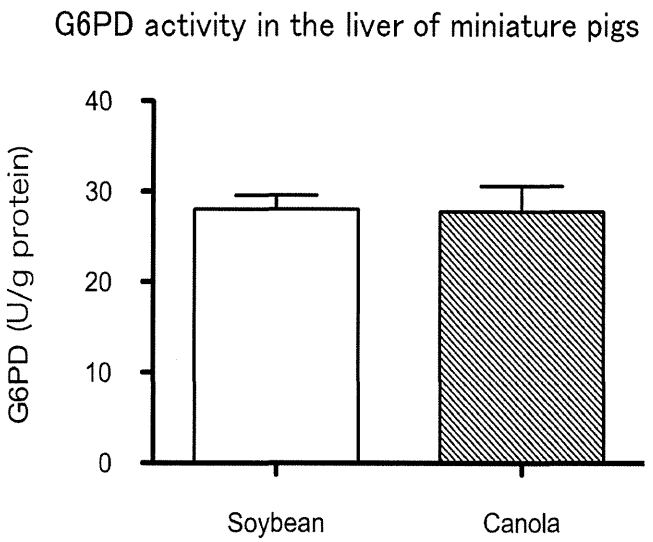

Figure 19　G6PD activity in the liver of miniature pigs

Male miniature pigs were fed on a diet added with 10 w/w% soybean oil or canola oil for 18 months. N=6.

III. 研究成果の刊行に関する一覧表

雑誌

発表者名	論文タイトル名	発表誌名	巻号	ページ	出版年
Ji X, Naito Y, Weng H, Endo K, Ma X, Iwai N	P2X7 deficiency attenuates hypertension and renal injury in deoxycorticosterone acetate-salt hypertension	Am J Physiol Renal Physiol	303	F1207-F1215	2012
Ji X, Naito Y, Weng H, Ma X, Endo K, Kito N, Yanagawa N, Yu Y, Li J, Iwai N	Renoprotective mechanisms of pirfenidone in hypertension-induced renal injury: through anti-fibrotic and anti-oxidative stress pathways	Biomed Res	34(6)	309-319	2013
Hashimoto Y, Yamada K, Tsushima H, Miyazawa D, Mori M, Nishio K, Ohkubo T, Hibino H, Ohara N, Okuyama H	Three dissimilar high fat diets differentially regulate lipid and glucose metabolism in obesity-resistant Slc:Wistar/ST rats	Lipids	48	803-815	2013

IV. 研究成果の刊行物・別刷

Am J Physiol Renal Physiol 303: F1207–F1215, 2012.
First published August 1, 2012; doi:10.1152/ajprenal.00051.2012.

$P2X_7$ deficiency attenuates hypertension and renal injury in deoxycorticosterone acetate-salt hypertension

Xu Ji, Yukiko Naito, Huachun Weng, Kosuke Endo, Xiao Ma, and Naoharu Iwai

Department of Genomic Medicine, National Cerebral and Cardiovascular Center, Suita, Japan

Submitted 27 January 2012; accepted in final form 26 July 2012

Ji X, Naito Y, Weng H, Endo K, Ma X, Iwai N. $P2X_7$ deficiency attenuates hypertension and renal injury in deoxycorticosterone acetate-salt hypertension. *Am J Physiol Renal Physiol* 303: F1207–F1215, 2012. First published August 1, 2012; doi:10.1152/ajprenal.00051.2012.—The $P2X_7$ receptor is a ligand-gated ion channel, and genetic variations in the $P2X_7$ gene significantly affect blood pressure. $P2X_7$ receptor expression is associated with renal injury and inflammatory diseases. Uninephrectomized wild-type (WT) and $P2X_7$-deficient ($P2X_7$ KO) mice were subcutaneously implanted with deoxycorticosterone acetate (DOCA) pellets and fed an 8% salt diet for 18 days. Their blood pressure was assessed by a telemetry system. The mice were placed in metabolic cages, and urine was collected for 24 h to assess renal function. After 18 days of DOCA-salt treatment, $P2X_7$ mRNA and protein expression increased in WT mice. Blood pressure in $P2X_7$ KO mice was less than that of WT mice (mean systolic blood pressure 133 ± 3 vs. 150 ± 2 mmHg). On *day 18*, urinary albumin excretion was lower in $P2X_7$ KO mice than in WT mice (0.11 ± 0.07 vs. 0.28 ± 0.07 mg/day). Creatinine clearance was higher in $P2X_7$ KO mice than in WT mice (551.53 ± 65.23 vs. 390.85 ± 32.81 $\mu l \cdot min^{-1} \cdot g$ renal $weight^{-1}$). Moreover, renal interstitial fibrosis and infiltration of immune cells (macrophages, T cells, B cells, and leukocytes) were markedly attenuated in $P2X_7$ KO mice compared with WT mice. The levels of IL-1β, released by macrophages, in $P2X_7$ KO mice had decreased dramatically compared with that in WT mice. These results strongly suggest that the $P2X_7$ receptor plays a key role in the development of hypertension and renal disease via increased inflammation, indicating its potential as a novel therapeutic target.

$P2X_7$; hypertension; renal injury; inflammation; immune cell

THE $P2X_7$ RECEPTOR is an ATP-gated cation channel (27), primarily expressed by various immune cells including macrophages (17, 20, 23) and lymphocytes (32, 33). Stimulation of this receptor leads to the release of IL-1β from macrophages (17, 20) and IL-2 from T cells (32, 33). The activation of macrophages and T cells in $P2X_7$-deficient ($P2X_7$ KO) mice is lower than that in wild-type (WT) mice (3, 28). The $P2X_7$ receptor plays a key role in inflammatory reactions, which are involved in various diseases (1, 7). Moreover, the $P2X_7$ receptor is involved in diverse renal disease models such as glomerular injury due to diabetes and hypertension (30), unilateral ureteral obstruction (10), renal injury due to salt-sensitive hypertension (13), and glomerulonephritis (29). Previously, we performed a genomewide quantitative trait locus analysis for rat blood pressure and found that the region around the *D12Arb6* marker (located near the $P2X_7$ gene) is involved in the regulation of blood pressure (12). It is also reported that $P2X_7$ genetic variation significantly affects blood pressure in a Caucasian population (19). Although the pathophysiology of hypertension and renal diseases is well studied (14, 31), few studies address the role of the $P2X_7$ receptor in the progression of hypertension and renal diseases. Therefore, the relevance of the $P2X_7$ receptor in hypertension and renal injury remains to be elucidated. Elucidating the factors responsible for deoxycorticosterone acetate (DOCA)-salt hypertension will enhance our understanding of the mechanisms of hypertension resulting from hypervolemia, hyperaldosteronism, and high salt intake. In the present study, we investigated the role of the $P2X_7$ receptor in the development of DOCA-salt hypertension and renal injury in WT and $P2X_7$ KO mice. We examined the possible effects of the $P2X_7$ receptor on blood pressure, renal function (i.e., urinary albumin and creatinine clearance), and renal injury (i.e., area of fibrosis). Furthermore, we investigated the possible effects of the $P2X_7$ receptor on infiltration of immune cells (i.e., macrophages, T cells, B cells, and leukocytes) in the kidneys and IL-1β release from macrophages. The possible effects of the $P2X_7$ receptor on cyclooxygenase-2 (COX-2) expression and total serum antioxidant activity were also examined in this study.

MATERIALS AND METHODS

Experimental animals. Male WT (C57BL/6J) mice were obtained from SLC Japan (Shizuoka, Japan), and male $P2X_7$ KO mice (26) were obtained from Jackson Laboratory (Bar Harbor, ME). $P2X_7$ KO mice were congenic with the C57BL/6J genetic background. The animals used in the experiments were 10–12 wk old. The mice were housed in a temperature-controlled pathogen-free room with light from 0700 to 1900 (daytime) and had free access to food and water. The experimental protocols were approved by the National Cerebral and Cardiovascular Center Committee for Laboratory Animals, and the care and use of the animals were performed in accordance with the National Institutes of Health *Guide for the Care and Use of Laboratory Animals.*

Measurement of blood pressure and expression of target mRNA in DOCA-salt hypertension mice. Before the DOCA-salt treatment, telemetry system transmitters (Data Sciences International, St. Paul, MN) were implanted (6). Both WT and $P2X_7$ KO mice were anesthetized with pentobarbital (25 mg/kg), and a transmitter catheter was inserted into the left carotid artery, with the transmitter body placed subcutaneously in the lower right side of the abdomen. Simultaneously, the left kidney was removed as baseline sample and cut longitudinally. One half of each kidney was frozen in liquid nitrogen, while the other half was fixed in 4% formalin.

Ten days after radiotelemetry implantation, mice were reanesthetized with pentobarbital (25 mg/kg), and a DOCA pellet (0.12 $mg \cdot g$ body $wt^{-1} \cdot day^{-1}$; Innovative Research of America, Sarasota, FL) was implanted subcutaneously in the neck region. Mice were fed an 8% NaCl diet, and the treatment with DOCA-salt was continued for 18 days.

Heart rate (HR), systolic blood pressure (SBP), diastolic blood pressure (DBP), and pulse pressure (PP) were measured throughout the DOCA-salt treatment period with the telemetry system according to the manufacturer's instructions. In addition, on *day 18*, mice were

Address for reprint requests and other correspondence: Y. Naito, Dept. of Genomic Medicine, National Cerebral and Cardiovascular Center, 5-7-1 Fujishirodai, Suita, Osaka 565-8565, Japan (e-mail: naitoy@ri.ncvc.go.jp).

housed for 24 h in metabolic cages to collect urine for measurement of albumin levels and creatinine clearance (C_{Cr}). Urine was stored at −80°C until renal function evaluation.

After the DOCA-salt treatment, mice were anesthetized with pentobarbital (25 mg/kg). Venous blood was collected from the vena cava. Plasma (EDTA as anticoagulant) and serum were isolated by centrifugation and stored at −80°C until measurement. The kidneys from each mouse were removed, weighed, and cut longitudinally. One half of each kidney was frozen in liquid nitrogen and used exclusively for the isolation of total RNA, while the other half was fixed in 4% formalin and used for histological analyses. Renal weight was expressed as renal organ weight per 10 g of body weight. RNA was isolated from the mouse kidneys with TRIzol reagent (Invitrogen, Carlsbad, CA). $P2X_7$ mRNA expression was measured by real-time RT-PCR analysis with commercial kits (Applied Biosystems, Foster City, CA); the levels were normalized to the expression of β-actin mRNA. Measurements are expressed as $\log_{10}[2^{35 - CT1}/2^{25 - CT2}]$, where $2^{35 - CT1}$ and $2^{25 - CT2}$ correspond to the expression levels of the target and β-actin mRNA, respectively.

Renal function assessment. A series of experiments were further performed to test the renal function of the $P2X_7$ KO mice with the same DOCA-salt diet treatment described above. Urine was collected for 24 h from mice in metabolic cages on *days 0*, *2*, *5*, *8*, and *18* to assess renal function.

Glomerular barrier function was determined by assessing urinary albumin excretion. The urinary albumin concentration was determined with an albumin enzyme-linked immunosorbent assay kit (Exocell; Shibayagi, Gunma, Japan).

Renal filtration function was evaluated by measuring C_{Cr} on *day 18*, which was calculated with the following formula: $C_{Cr} = (U_{Cr} \times V)/P_{Cr}/KW$, where U_{Cr} is the concentration of urinary creatinine (mg/dl), P_{Cr} is the concentration of plasma creatinine (mg/dl), V is the urine flow rate (μl/min), and KW is the weight of the kidney (g). Creatinine levels were measured with a QuantiChrom creatinine assay kit (DIUR-500; Bioassay Systems, Hayward, CA). Urinary sodium concentration was measured with a compact salt meter (C-121; Horiba, Kyoto, Japan). Urine samples of mice in the telemetry examination were also used to measure urinary volume, albumin level, and C_{Cr} on *day 18*.

Histological examination. Tubulointerstitial injury in the renal cortex was measured as the percentage of the area of fibrosis and estimated by Sirius red staining. The formaldehyde-fixed kidneys were embedded in paraffin before sections were prepared and stained with Sirius red. For each kidney, 10 microscopic fields (×400 magnification) were chosen randomly with a fluorescence microscope (BZ-9000; Keyence, Osaka, Japan), the area of renal fibrosis was measured and analyzed with analysis software (BZ image analyzer II; Keyence), and the mean value was calculated for each kidney.

Immunohistochemistry. Immunohistochemistry was used to detect $P2X_7$, macrophages, T cells, B cells, leukocytes, and podocytes. Paraffin sections were deparaffinized with xylene in a graded-alcohol series. After antigen retrieval, endogenous peroxidase activity was blocked by incubation in 3.3% H_2O_2 at room temperature for 30 min, followed by incubation in 5% normal goat serum for 1 h to block nonspecific binding. After thorough washing with phosphate-buffered saline (PBS), the sections were incubated overnight at 4°C with primary antibodies against $P2X_7$ (Alomone Labs, Jerusalem, Israel), F4/80 (Santa Cruz Biotechnology, Santa Cruz, CA), CD3 (DAKO, Glostrup, Denmark), CD20 (eBioscience, San Diego, CA), CD45 (BD Pharmingen, San Diego, CA), synaptopodin (Santa Cruz Biotechnology), and COX-2 (Cayman Chemical, Ann Arbor, MI). The Simplestain MAX-PO (mouse) kit (Nichirei, Tokyo, Japan) was used as a secondary antibody and incubated for 30 min at room temperature. Antibody binding was visualized with 3,3′-diaminobenzidine (DAB; Dojindo Laboratories, Kumamoto, Japan), and the nuclei were stained with hematoxylin. Images were captured at high-power magnification (×400) in 10 fields for each kidney with a fluorescence microscope (BZ-9000, Keyence). The numbers of positive cells were counted, and the results were expressed as the number of positive cells per square millimeter of kidney tissue. To determine the relationship between $P2X_7$ receptors and macrophages in WT mice after DOCA-salt treatment, the expression sites of $P2X_7$ and F4/80 in consecutive sections were observed. In addition, to determine the relationship between $P2X_7$ receptors and podocytes in WT mice after DOCA-salt treatment, colocalization studies on $P2X_7$ and synaptopodin (a podocyte marker) in consecutive sections were performed.

Assessment of IL-1β secretion by macrophages. Peritoneal macrophages were collected as described previously (3, 13). Briefly, mice

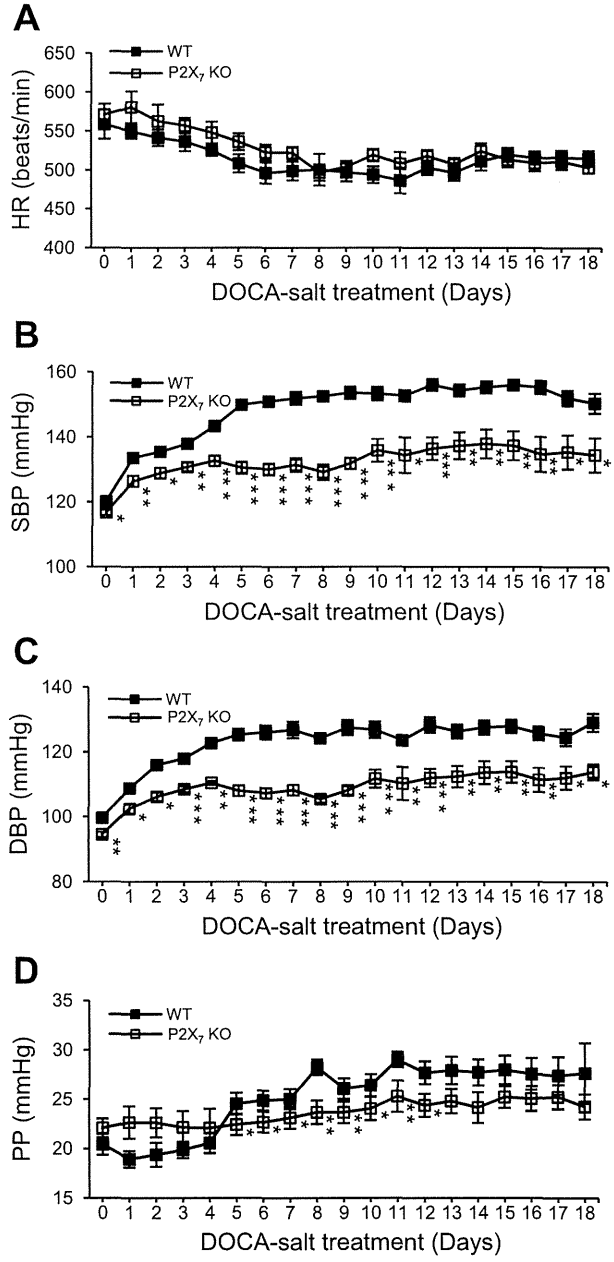

Fig. 1. Effects of $P2X_7$ deletion on heart rate (HR), systolic blood pressure (SBP), diastolic blood pressure (DBP), and pulse pressure (PP) in response to DOCA-salt treatment. HR (*A*), SBP (*B*), DBP (*C*), and PP (*D*) in WT (n = 8) and $P2X_7$-deficient ($P2X_7$ KO; n = 8) mice were measured for 24 h with a telemetry system. SBP, DBP, and PP were lower in $P2X_7$ KO mice than in WT mice; average SBP, DBP, and PP were also lower in $P2X_7$ KO mice than in WT mice. *$P < 0.05$, **$P < 0.01$, ***$P < 0.001$, significantly different from WT mice (unpaired Student's t-test).

(WT and P2X7 KO, n = 10, fed a normal diet) were injected intraperitoneally with 3% sterile thioglycollate medium (BD Diagnostic Systems, Sparks, MD), and 4 days later the peritoneal exudate corpuscles were collected by lavage with PBS. Cell suspensions were seeded in 12-well cell culture plates (2×10^6 cells/well) in RPMI 1640 medium (Nacalai Tesque, Kyoto, Japan) containing 10% fetal bovine serum (Thermo Scientific Hyclone, Logan, UT) and 2 mM L-glutamine (GIBCO-BRL, Grand Island, NY) (2 wells for each sample). After 4 h of incubation at 37°C in a 5% CO_2 atmosphere, nonadherent cells were removed with fresh RPMI 1640 medium. After incubation for 48 h at 37°C, to accumulate IL-1β in macrophages, these cells were then primed with 10 ng/ml lipopolysaccharide (LPS, recombinant source from *Escherichia coli*, serotype 0111: B4; Sigma-Aldrich, Poole, UK) for 24 h at 37°C. To assess IL-1β release, the LPS-stimulated cells were stimulated for 6 h with 100 μM BzATP, a P2X7 agonist that is a mixture of 2′- and 3′-*O*-(4-benzoylbenzoyl)adenosine 5′-triphosphate (Sigma, St. Louis, MO). Cells treated with vehicle (PBS) served as negative controls. The media were then transferred to new tubes and centrifuged at 14,000 rpm for 10 min at 4°C to remove any nonadherent cells. The clear supernatants were stored at −80°C until use. Mouse IL-1β was measured in duplicate with an enzyme-linked immunosorbent assay kit (Thermo Scientific, Rockford, IL).

Spectrophotometric assay for determination of total serum antioxidant activity. To evaluate the ability of reactive oxygen species, we measured the total serum antioxidant activity by using a total antioxidant power colorimetric microplate assay kit (Oxford Biomedical Research, Oxford, MI). This assay measures reductive capacity by detecting the reduction of Cu^{2+} to Cu^{+}.

Statistical analysis. Values are expressed as means ± SE. Statistical analyses were performed with JMP (SAS Institute, Cary, NC). Analysis of variance (ANOVA) was used to estimate differences among groups, and the significance of differences was tested with Student's *t*-test.

RESULTS

HR and blood pressure. Baseline values of HR and PP (before DOCA-salt treatment) in the WT mice were not significantly different from those in the P2X7 KO mice. However, the basal SBP and DBP values were significantly different between the two groups, although the difference was small [SBP: 120.1 ± 1.2 vs. 116.7 ± 0.8 mmHg ($P < 0.05$), DBP: 99.7 ± 0.1 vs. 94.6 ± 0.8 mmHg ($P < 0.01$), WT vs. P2X7 KO, respectively] (Fig. 1).

There were no significant differences in HR between WT and P2X7 KO mice during the DOCA-salt treatment period. Blood pressure of the WT mice increased progressively during the DOCA-salt treatment period, peaking on *day 5* (mean SBP and DBP from *days 5–18*: 153.2 ± 1.9 and 126.4 ± 1.9 mmHg, respectively). DOCA-salt treatment resulted in steady markedly high levels of SBP, DBP, and PP from *day 5* in the WT mice; however, these parameters only increased marginally in the P2X7 KO mice ($P < 0.0001$ with ANOVA; Fig. 1).

Renal function. Glomerular barrier function was determined by assessing urinary albumin concentrations during the DOCA-salt treatment period (Fig. 2*A*), and renal filtration function was evaluated by measuring C_{Cr} on *day 18* of the treatment (Fig. 2*B*).

Baseline urinary albumin levels were similar in WT and P2X7 KO mice. Urinary albumin levels increased progressively during the DOCA-salt treatment period in the WT mice.

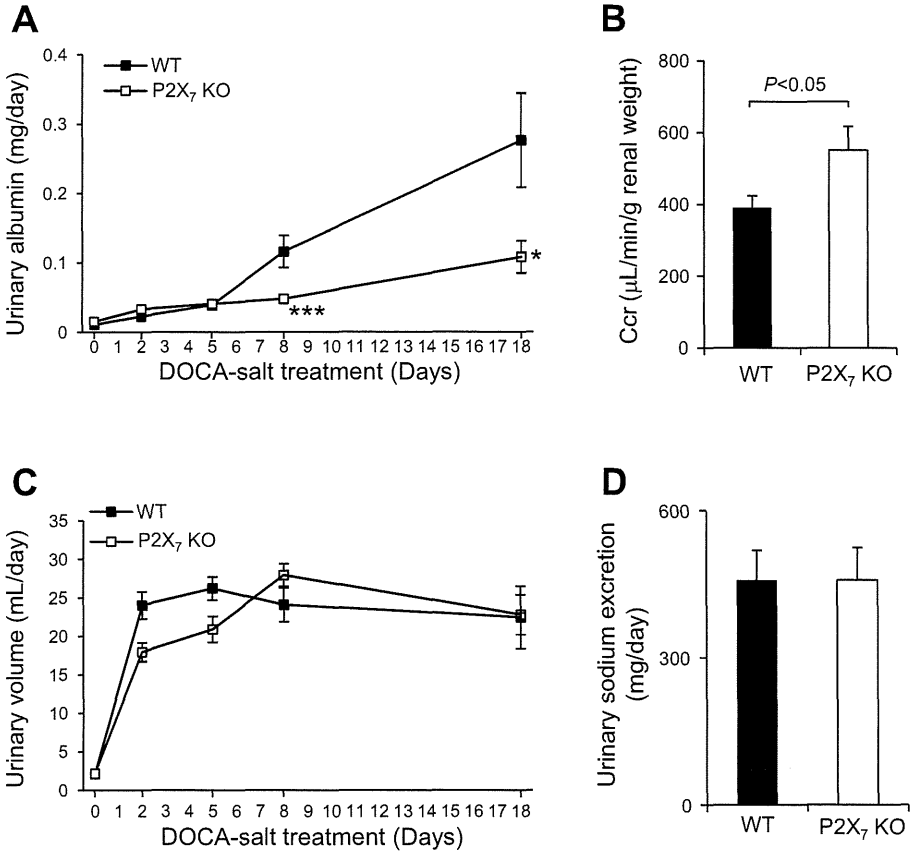

Fig. 2. Effects of P2X7 deletion on renal function in response to DOCA-salt treatment: urinary albumin (*A*), creatinine clearance (C_{Cr}; *B*), urinary volume (*C*), and urinary sodium excretion (*D*) in WT and P2X7 KO mice. n = 10 for WT and n = 8 for P2X7 KO mice in *A* and *C*; n = 18 for WT and n = 16 for P2X7 KO mice in *B* and *D*. *$P < 0.05$, ***$P < 0.001$, significantly different from WT mice (unpaired Student's *t*-test).

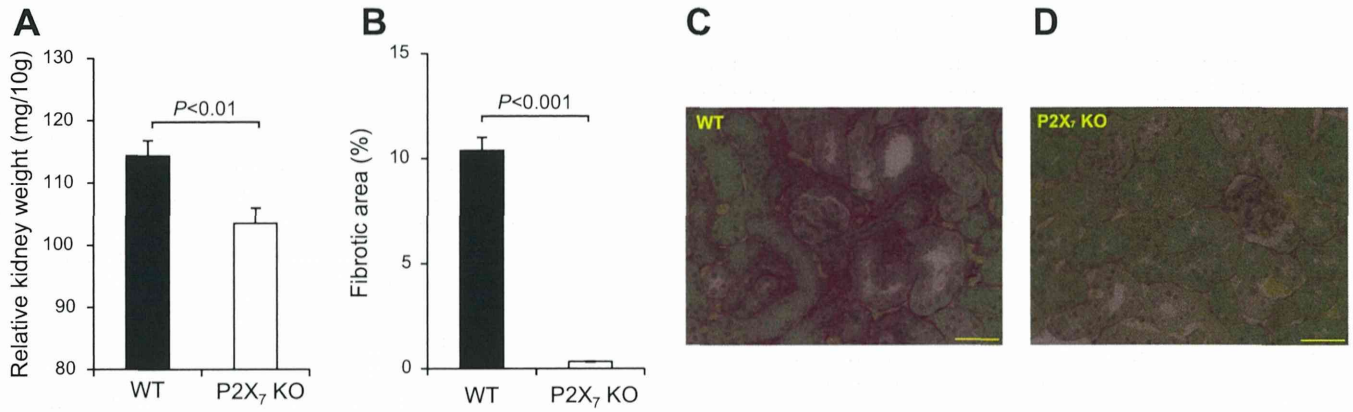

Fig. 3. Effects on interstitial fibrosis due to DOCA-salt hypertension in $P2X_7$ KO mice. *A*: relative renal weight in WT (n = 18) and $P2X_7$ KO (n = 16) mice; values represent renal organ weight per 10 g body weight. *B*: % of interstitial fibrosis area 18 days after DOCA-salt treatment in WT (n = 8) and $P2X_7$ KO (n = 8) mice. *C* and *D*: representative images of the kidneys of WT (*C*) and $P2X_7$ KO (*D*) mice stained with Sirius red show interstitial fibrosis (red-colored area). WT mice exhibited significantly larger areas of interstitial fibrosis than $P2X_7$ KO mice. Scale bars, 50 μm.

However, on *days 8* and *18*, the urinary albumin levels in the $P2X_7$ KO mice were lower than those in the WT mice ($P < 0.001$ and $P < 0.05$ on *days 8* and *18*, respectively). On *day 18*, the urinary albumin measurements of the $P2X_7$ KO and WT mice were 0.11 ± 0.07 and 0.28 ± 0.07 mg/day, respectively. On *day 18*, C_{Cr} was significantly higher in the $P2X_7$ KO mice than in the WT mice ($P < 0.05$; Fig. 2*B*). However, there were no significant differences in urinary volume (Fig. 2*C*) or sodium excretion (Fig. 2*D*) between WT and $P2X_7$ KO mice.

On *day 18*, the renal weight of the $P2X_7$ KO mice was lower than that of the WT mice ($P < 0.01$; Fig. 3*A*). Histological examination detected renal interstitial fibrosis in both WT and $P2X_7$ KO mice (Fig. 3, *C* and *D*); however, it was attenuated in $P2X_7$ KO mice compared with WT mice on *day 18* of DOCA-salt treatment ($P < 0.001$; Fig. 3*B*).

$P2X_7$ expression response to DOCA-salt treatment. Immunohistochemical analysis of renal $P2X_7$ revealed that the number of $P2X_7$-positive cells increased significantly in WT mice after DOCA-salt treatment (Fig. 4*C*) compared with that in untreated WT mice (Fig. 4*A*). However, $P2X_7$-positive cells were undetectable under all conditions in $P2X_7$ KO mice (Fig. 4, *B* and *D*). The numbers of $P2X_7$-positive cells are shown in Fig. 4*E*. Similar results were obtained for the expression of $P2X_7$ mRNA ($P < 0.05$; Fig. 4*F*).

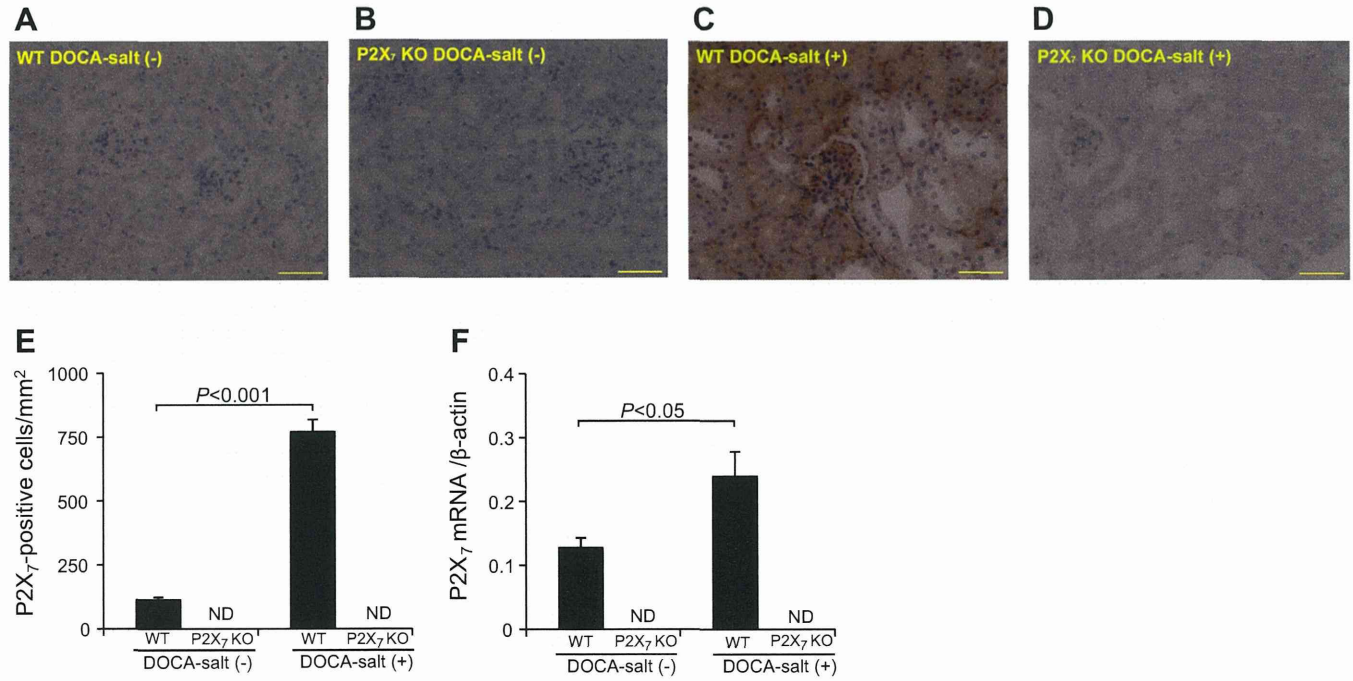

Fig. 4. Effects of DOCA-salt treatment on $P2X_7$ expression in the kidneys. The number of $P2X_7$-positive cells increased significantly in DOCA-salt treated WT mice (*C*) compared with untreated WT mice (*A*). No $P2X_7$-positive cells were detected in either untreated (*B*) or DOCA-salt treated (*D*) $P2X_7$ KO mice. Mice without DOCA-salt treatment are designated DOCA-salt(−); DOCA-salt treatment after 18 days is designated DOCA-salt(+). *E*: average number of $P2X_7$-positive cells per mm^2 in WT and $P2X_7$ KO mice with and without DOCA-salt treatment. *F*: expression levels of $P2X_7$ mRNA in WT and $P2X_7$ KO mice with and without DOCA-salt treatment. Values are ratios relative to those of β-actin. ND, not detected (n = 8 for WT and $P2X_7$ KO mice). Scale bars, 50 μm.

Renal inflammatory response expression after DOCA-salt treatment. Immunohistochemical analysis of the kidneys revealed that infiltration of macrophages (F4/80-positive cells), T cells (CD3-positive cells), B cells (CD20-positive cells), and leukocytes (CD45-positive cells) was also markedly attenuated in P2X$_7$ KO mice compared with that in WT mice ($P < 0.001$; Fig. 5).

Expression site studies in consecutive sections were carried out to determine the relationship between P2X$_7$ and macrophages in the kidneys. P2X$_7$ receptor immunoreactivity was colocalized with positive macrophages (Fig. 6).

To determine the relationship between P2X$_7$ receptors and podocytes, colocalization studies of P2X$_7$ and podocytes in consecutive sections were performed. P2X$_7$ receptor immunoreactivity was colocalized with positive synaptopodin (a podocyte marker) in the glomeruli (Fig. 7).

IL-1β release from WT and P2X$_7$ KO mouse macrophages. To confirm the capacity for IL-1β release mediated by P2X$_7$ receptor stimulation, peritoneal macrophages from WT and P2X$_7$ KO mice were primed with LPS and then stimulated with the P2X$_7$ agonist BzATP. In the presence of LPS only, IL-1β was released from neither WT nor P2X$_7$ KO mouse macrophages. However, in the presence of LPS and BzATP, IL-1β was released from the WT mouse macrophages but not from the P2X$_7$ KO mouse macrophages ($P < 0.001$; Fig. 8).

Effects of DOCA-salt treatment on COX-2 expression in the kidneys. Immunohistochemical examination of the kidney tissues revealed that, on *day 18* of DOCA-salt treatment, the

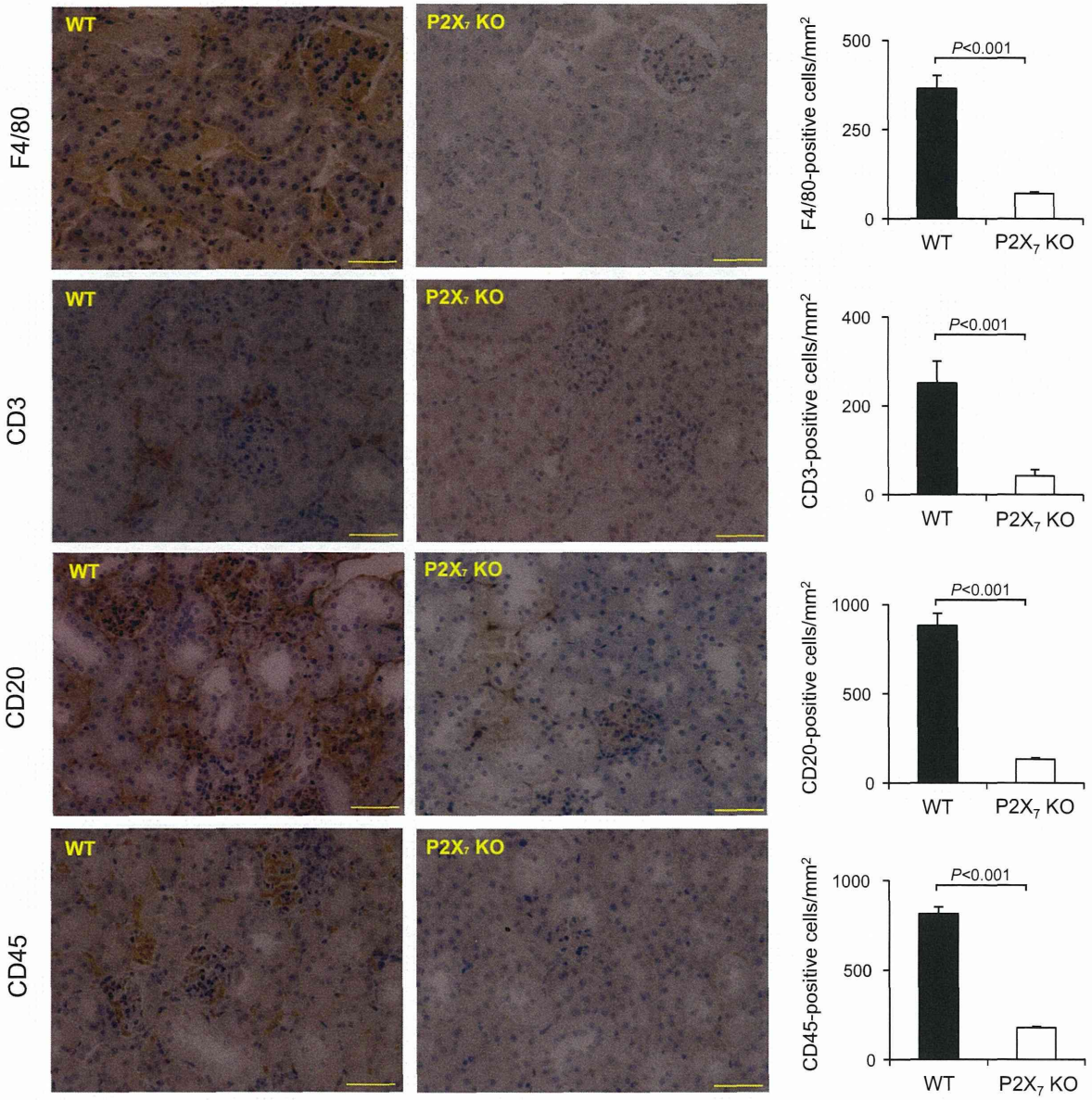

Fig. 5. Effects of DOCA-salt treatment on immune cell infiltration in the kidneys. The infiltration of macrophages (F4/80-positive cells), T cells (CD3-positive cells), B cells (CD20-positive cells), and leukocytes (CD45-positive cells) was measured by immunohistochemistry. There were significantly greater numbers of these immune cells in the kidneys of WT mice than those of P2X$_7$ KO mice. The average numbers of immune cells per mm^2 on *day 18* after DOCA-salt treatment in WT and P2X$_7$ KO mice are also shown. However, immune cell infiltration was significantly attenuated in P2X$_7$ KO mice compared with WT mice ($n = 8$ for WT and P2X$_7$ KO mice). Scale bars, 50 μm.

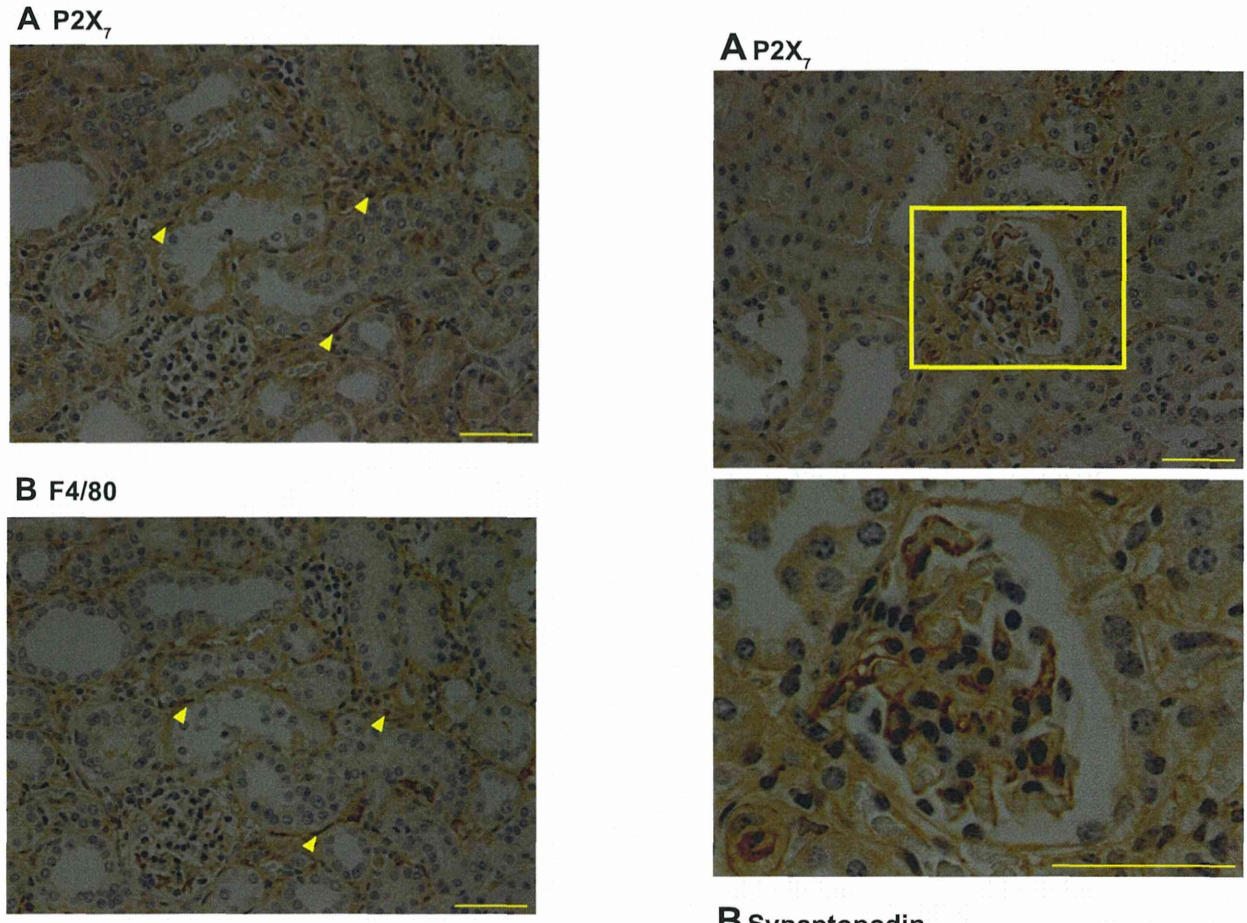

Fig. 6. Typical photographs of $P2X_7$ and F4/80 (a macrophage marker) colocalization in consecutive renal sections from WT mice. Immunohistochemical examination identified $P2X_7$ and macrophages by positive staining with anti-$P2X_7$ (*A*) and anti-F4/80 (*B*) antibodies, respectively. Macrophages coexpressed with $P2X_7$ are shown by arrowheads. Scale bars, 50 μm.

expression levels of COX-2 protein in the kidneys of $P2X_7$ KO mice were markedly lower than the corresponding levels in WT mice (Fig. 9).

Effects of DOCA-salt treatment on total serum antioxidant activity. To evaluate the ability of reactive oxygen species, the total serum antioxidant activity (expressed as copper reducing equivalents) was measured. The level of activity was significantly higher in $P2X_7$ KO mice than in WT mice on *day 18* of DOCA-salt treatment (Fig. 10).

DISCUSSION

The $P2X_7$ receptor plays a key role in the modulation of inflammatory processes (1, 7, 15, 16). Indeed, the $P2X_7$ receptor is involved in various hypertension (12, 19) and renal (10,

Fig. 7. Typical photographs of $P2X_7$ and synaptopodin (a podocyte marker) colocalization in consecutive renal sections from WT mice. Immunohistochemical examination identified $P2X_7$ and macrophages by positive staining with anti-$P2X_7$ (*A*) and anti-synaptopodin (*B*) antibodies, respectively. Podocytes coexpressed with $P2X_7$ are shown. *Bottom*: magnified photographs of rectangular areas shown at *top*. Scale bars, 50 μm.

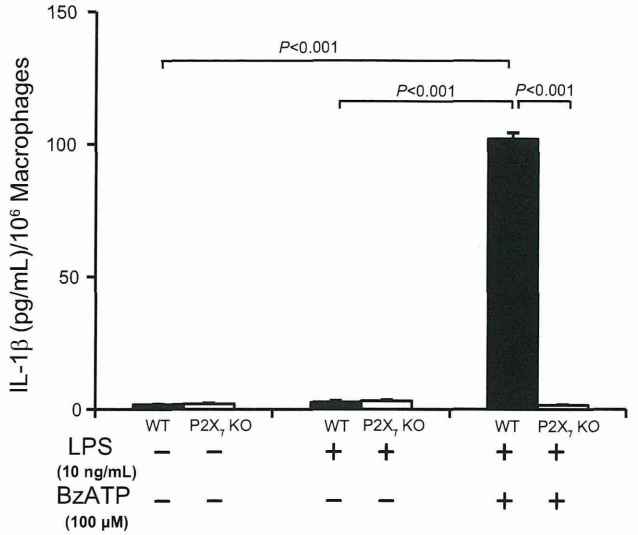

Fig. 8. IL-1β release from peritoneal macrophages of WT and $P2X_7$ KO mice, mediated by $P2X_7$ receptor stimulation. Peritoneal macrophages from WT and P2X7 KO mice were primed with LPS and then stimulated with the P2X7 agonist BzATP. In the presence of LPS only, IL-1β was released from neither WT nor P2X7 KO mouse macrophages. However, IL-1β was released from the WT mouse macrophages but not from the $P2X_7$ KO mouse macrophages in response to LPS + BzATP treatment (n = 10 for WT and $P2X_7$ KO mice).

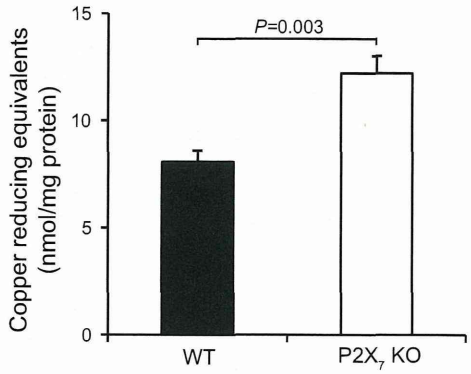

Fig. 10. Effects of DOCA-salt treatment on total serum antioxidant activity. Total serum antioxidant activity was measured with a total antioxidant power kit. The level of activity (expressed as copper reducing equivalents) was significantly higher in $P2X_7$ KO mice than that in WT mice on *day 18* of DOCA-salt treatment (n = 10 for WT and $P2X_7$ KO mice).

13, 29, 30) diseases. However, its functional role in hypertension and renal injury remains unclear.

In the present study, deletion of the $P2X_7$ gene ameliorated hypertension and renal function by reducing renal injury and inflammation. Specifically, renal injury was attenuated as reflected by reduced urinary albumin levels, renal interstitial fibrosis, and increased C_{Cr} levels. In addition, renal inflammation was also reduced, as determined by decreased inflammatory cell infiltration (i.e., macrophages, T cells, B cells, and leukocytes). Moreover, IL-1β was released by the WT mouse macrophages but not by the $P2X_7$ KO mouse macrophages. These results strongly suggest that $P2X_7$ is involved in hypertension and renal injury via renal inflammatory responses.

Although only minimally, the lower baseline blood pressure of the $P2X_7$ KO mice was significantly different from that of the WT mice. This suggests that the $P2X_7$ receptor contributes minimally to baseline blood pressure. Renal $P2X_7$ mRNA and protein expression were significantly upregulated in WT mice after DOCA-salt treatment; this upregulation may be related to elevated blood pressure in WT mice. Furthermore, DOCA-salt treatment elevated the blood pressure of WT mice, but this elevation was significantly attenuated in $P2X_7$ KO mice.

Chronic hypertension is a major risk factor for end-stage renal disease (2, 4). Furthermore, there is a greater incidence of end-stage renal disease in patients with salt-sensitive hypertension (22). In the present study, urinary sodium excretion was not significantly different between WT and $P2X_7$ KO mice, suggesting that the same amount of sodium is excreted in both types of mice after high salt intake. Urinary albumin excretion increased significantly in the WT mice after DOCA-salt treatment, but this increase was strongly attenuated in the $P2X_7$ KO mice. C_{Cr} levels were much higher in the $P2X_7$ KO mice than in the WT mice, and the renal weight of the $P2X_7$ KO mice was lower than that of the WT mice. In $P2X_7$ KO mice, renal injury was alleviated, a further increase in renal weight was inhibited, and C_{Cr} levels also increased because of improved renal function. Therefore, C_{Cr} levels are inversely related to renal weight. These results suggest that $P2X_7$ receptor deficiency protects renal function during DOCA-salt hypertension.

We aimed to determine how $P2X_7$ affects DOCA-salt hypertension and renal injury. Stimulation of the $P2X_7$ receptor is reported to cause the release of inflammatory cytokines from macrophages and lymphocytes (1, 17, 20, 32, 33). In addition, macrophage and T-cell infiltration in the kidneys is regarded as a key event in renal injury, leading to renal fibrosis and

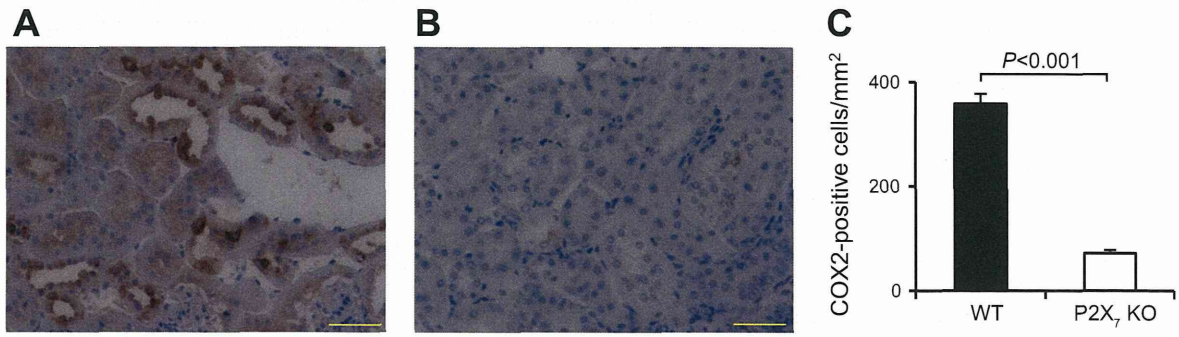

Fig. 9. Effects of DOCA-salt treatment on COX-2 expression in the kidneys. *A* and *B*: positive cell numbers of COX-2 were significantly higher in WT mice (*A*) than in $P2X_7$ KO mice (*B*) on *day 18* of DOCA-salt treatment. *C*: average positive cell number of COX-2 per mm^2 in WT and $P2X_7$ KO mice on *day 18* of DOCA-salt treatment. (n = 8 for WT and $P2X_7$ KO mice). Scale bars, 50 μm.

proteinuria (7, 15, 16). Recent reports also suggest that renal infiltration involving immune cells plays a role in the pathogenesis of hypertension (5, 18, 21). Therefore, in the present study, to address the aforementioned issue, the infiltration of immune cells (i.e., macrophages, T cells, B cells, and leukocytes) was measured by immunohistochemistry. Immune cell infiltration increased significantly in the WT mice after DOCA-salt treatment, but this increase was significantly smaller in the $P2X_7$ KO mice. Furthermore, the colocalization of $P2X_7$ and F4/80 (a macrophage marker) was observed in consecutive renal sections. These results suggest that renal $P2X_7$ expression may be correlated with the inflammatory pathway via the stimulation of immune cells.

Although immune cells are reported to play a deleterious role in both the hypertension and renal injury associated with DOCA-salt hypertension (5), the mechanisms by which immune cells are involved in hypertension and renal injury are unclear. We confirmed the capacity of the peritoneal macrophages of WT and $P2X_7$ KO mice to release IL-1β mediated by $P2X_7$ receptor stimulation. After LPS and BzATP stimulation, IL-1β was released from WT mouse macrophages but not from $P2X_7$ KO mouse macrophages. These results suggest that the release of the inflammatory cytokine IL-1β by macrophages is related to the $P2X_7$ receptor. Inflammatory responses were attenuated in immune cells deficient in $P2X_7$, which subsequently attenuated inflammatory responses preventing renal injury, which in turn led to lower blood pressure. Therefore, this study revealed that the $P2X_7$ receptors of immune cells play important roles in renal injury and hypertension. The activation of macrophages and T cells in $P2X_7$ KO mice is reported to be lower than that in WT mice (3, 28). The results of these reports also support our hypothesis. In addition, $P2X_7$ deficiency also affected downstream effectors of IL-1β signaling, such as COX-2 and reactive oxygen species.

Initially, DOCA-salt treatment increased blood pressure slightly; this initial slight increase in blood pressure could induce minimal renal injury, which may have increased the inflammatory reaction. In turn, the inflammatory reaction may be related to the $P2X_7$ pathway of immune cells, which could then lead to progressively worsening renal function, resulting in moderate hypertension. Moreover, such renal injury is likely to initiate a vicious cycle of hypertension, resulting in greater nephron loss and blood pressure. The $P2X_7$ receptor did not affect the initial slight increase in blood pressure because blood pressure until *day 4* was slightly elevated in both $P2X_7$ KO and WT mice after DOCA-salt treatment. Therefore, the $P2X_7$ receptor attenuates only the vicious cycle of hypertension and renal injury via immune cells. The inflammatory reaction plays an important role via the $P2X_7$ pathway of immune cells in this vicious cycle between renal injury and hypertension.

The causes of hypertension and renal injury are very complicated. A recent report suggests that the $P2X_7$ receptor is involved in thrombosis (9). As thrombosis of the kidneys may beget renal injury, it is also a possible cause of hypertension and renal injury. Furthermore, several studies report that the $P2X_7$ receptor is expressed in glomerular mesangial cells (11, 24, 30), podocytes (8, 30), and medullary collecting duct cells (25). We also found that the $P2X_7$ receptor is expressed in podocytes by examining the immunohistochemistry of $P2X_7$-synaptopodin (a podocyte marker) colocalization. The $P2X_7$ receptor of these cells might also be involved in the regulation of blood pressure and renal function. However, further studies are needed to investigate these speculations.

In conclusion, our results demonstrate the following: elevated $P2X_7$ levels evoke sustained renal inflammation, which could lead to the development of hypertension and renal injury; $P2X_7$ deficiency prevents the development of hypertension and renal injury; and there is a positive relationship between the $P2X_7$ gene and hypertension. Our results suggest that $P2X_7$ plays important roles in the development and progression of hypertension and renal injury. Moreover, the $P2X_7$ receptor may be an important novel therapeutic target in hypertension-induced renal injury. This study contributes to a better understanding of mechanisms, prevention, and therapies for hypertension and renal injury.

ACKNOWLEDGMENTS

We express our gratitude to Dr. Go Hirokawa, Dr. Yumiko Hiura, and Dr. Rie Takahashi for their helpful suggestions.

GRANTS

This work was supported in part by the Program for the Promotion of Fundamental Studies in Health Science of the National Institute of Biomedical Innovation, Japan (Project ID: 10–24); a Grant-in-Aid for Scientific Research (C), Japan (23590705); the Adaptable and Seamless Technology Transfer Program through Target-driven R&D, Japan (AS232Z02131G); Health and Labour Sciences Research Grants, Japan (H24-food-004); and the Advanced Research for Medical Products Mining Programme of the National Institute of Biomedical Innovation (NIBIO), Japan.

DISCLOSURES

No conflicts of interest, financial or otherwise, are declared by the author(s).

AUTHOR CONTRIBUTIONS

Author contributions: X.J., Y.N., and N.I. conception and design of research; X.J., Y.N., H.W., K.E., and X.M. performed experiments; X.J., Y.N., H.W., K.E., and X.M. analyzed data; X.J., Y.N., and N.I. interpreted results of experiments; X.J., Y.N., and N.I. prepared figures; X.J., Y.N., and N.I. drafted manuscript; X.J., Y.N., and N.I. edited and revised manuscript; X.J., Y.N., and N.I. approved final version of manuscript.

REFERENCES

1. **Arulkumaran N, Unwin RJ, Tam FW.** A potential therapeutic role for P2X7 receptor (P2X7R) antagonists in the treatment of inflammatory diseases. *Expert Opin Investig Drugs* 20: 897–915, 2011.
2. **Barri YM.** Hypertension and kidney disease: a deadly connection. *Curr Hypertens Rep* 10: 39–45, 2008.
3. **Basso AM, Bratcher NA, Harris RR, Jarvis MF, Decker MW, Rueter LE.** Behavioral profile of P2X7 receptor knockout mice in animal models of depression and anxiety: relevance for neuropsychiatric disorders. *Behav Brain Res* 198: 83–90, 2009.
4. **Bidani AK, Griffin KA.** Pathophysiology of hypertensive renal damage: implications for therapy. *Hypertension* 44: 595–601, 2004.
5. **Boesen EI, Williams DL, Pollock JS, Pollock DM.** Immunosuppression with mycophenolate mofetil attenuates the development of hypertension and albuminuria in deoxycorticosterone acetate-salt hypertensive rats. *Clin Exp Pharmacol Physiol* 37: 1016–1022, 2010.
6. **Chen CS, Hiura Y, Shen CS, Iwai N.** Assessment of mitochondrial DNA polymorphisms in salt-sensitive hypertension in Dahl salt-sensitive rats. *Hypertens Res* 31: 107–115, 2008.
7. **Ferrari D, Pizzirani C, Adinolfi E, Lemoli RM, Curti A, Idzko M, Panther E, Di Virgilio F.** The P2X7 receptor: a key player in IL-1 processing and release. *J Immunol* 176: 3877–3883, 2006.
8. **Fischer KG, Saueressig U, Jacobshagen C, Wichelmann A, Pavenstadt H.** Extracellular nucleotides regulate cellular functions of podocytes in culture. *Am J Physiol Renal Physiol* 281: F1075–F1081, 2001.
9. **Furlan-Freguia C, Marchese P, Gruber A, Ruggeri ZM, Ruf W.** P2X7 receptor signaling contributes to tissue factor-dependent thrombosis in mice. *J Clin Invest* 121: 2932–2944, 2011.

10. **Goncalves RG, Gabrich L, Rosario A Jr, Takiya CM, Ferreira ML, Chiarini LB, Persechini PM, Coutinho-Silva R, Leite M Jr.** The role of purinergic P2X7 receptors in the inflammation and fibrosis of unilateral ureteral obstruction in mice. *Kidney Int* 70: 1599–1606, 2006.
11. **Harada H, Chan CM, Loesch A, Unwin R, Burnstock G.** Induction of proliferation and apoptotic cell death via P2Y and P2X receptors, respectively, in rat glomerular mesangial cells. *Kidney Int* 57: 949–958, 2000.
12. **Iwai N, Yasui N, Naraba H, Tago N, Yamawaki H, Sumiya H.** Klk1 as one of the genes contributing to hypertension in Dahl salt-sensitive rat. *Hypertension* 45: 947–953, 2005.
13. **Ji X, Naito Y, Hirokawa G, Weng H, Hiura Y, Takahashi R, Iwai N.** P2X$_7$ receptor antagonism attenuates the hypertension and renal injury in Dahl salt-sensitive rats. *Hypertens Res* 35: 173–179, 2012.
14. **Kajimoto K, Hiura Y, Sumiya T, Yasui N, Okuda T, Iwai N.** Exclusion of the catechol-*o*-methyltransferase gene from genes contributing to salt-sensitive hypertension in Dahl salt-sensitive rats. *Hypertens Res* 30: 459–467, 2007.
15. **Labasi JM, Petrushova N, Donovan C, McCurdy S, Lira P, Payette MM, Brissette W, Wicks JR, Audoly L, Gabel CA.** Absence of the P2X7 receptor alters leukocyte function and attenuates an inflammatory response. *J Immunol* 168: 6436–6445, 2002.
16. **Lister MF, Sharkey J, Sawatzky DA, Hodgkiss JP, Davidson DJ, Rossi AG, Finlayson K.** The role of the purinergic P2X7 receptor in inflammation. *J Inflamm* 4: 5, 2007.
17. **MacKenzie A, Wilson HL, Kiss-Toth E, Dower SK, North RA, Surprenant A.** Rapid secretion of interleukin-1beta by microvesicle shedding. *Immunity* 15: 825–835, 2001.
18. **Nava M, Quiroz Y, Vaziri N, Rodriguez-Iturbe B.** Melatonin reduces renal interstitial inflammation and improves hypertension in spontaneously hypertensive rats. *Am J Physiol Renal Physiol* 284: F447–F454, 2003.
19. **Palomino-Doza J, Rahman TJ, Avery PJ, Mayosi BM, Farrall M, Watkins H, Edwards CR, Keavney B.** Ambulatory blood pressure is associated with polymorphic variation in P2X receptor genes. *Hypertension* 52: 980–985, 2008.
20. **Qu Y, Franchi L, Nunez G, Dubyak GR.** Nonclassical IL-1beta secretion stimulated by P2X7 receptors is dependent on inflammasome activation and correlated with exosome release in murine macrophages. *J Immunol* 179: 1913–1925, 2007.
21. **Rodriguez-Iturbe B, Quiroz Y, Nava M, Bonet L, Chavez M, Herrera-Acosta J, Johnson RJ, Pons HA.** Reduction of renal immune cell infiltration results in blood pressure control in genetically hypertensive rats. *Am J Physiol Renal Physiol* 282: F191–F201, 2002.
22. **Rostand SG, Kirk KA, Rutsky EA, Pate BA.** Racial differences in the incidence of treatment for end-stage renal disease. *N Engl J Med* 306: 1276–1279, 1982.
23. **Sanz JM, Chiozzi P, Di Virgilio F.** Tenidap enhances P2Z/P2X7 receptor signalling in macrophages. *Eur J Pharmacol* 355: 235–244, 1998.
24. **Schulze-Lohoff E, Hugo C, Rost S, Arnold S, Gruber A, Brune B, Sterzel RB.** Extracellular ATP causes apoptosis and necrosis of cultured mesangial cells via P2Z/P2X7 receptors. *Am J Physiol Renal Physiol* 275: F962–F971, 1998.
25. **Schwiebert EM, Kishore BK.** Extracellular nucleotide signaling along the renal epithelium. *Am J Physiol Renal Physiol* 280: F945–F963, 2001.
26. **Solle M, Labasi J, Perregaux DG, Stam E, Petrushova N, Koller BH, Griffiths RJ, Gabel CA.** Altered cytokine production in mice lacking P2X$_7$ receptors. *J Biol Chem* 276: 125–132, 2001.
27. **Surprenant A, Rassendren F, Kawashima E, North RA, Buell G.** The cytolytic P2Z receptor for extracellular ATP identified as a P2X receptor (P2X7). *Science* 272: 735–738, 1996.
28. **Taylor SR, Gonzalez-Begne M, Sojka DK, Richardson JC, Sheardown SA, Harrison SM, Pusey CD, Tam FW, Elliott JI.** Lymphocytes from P2X7-deficient mice exhibit enhanced P2X7 responses. *J Leukoc Biol* 85: 978–986, 2009.
29. **Taylor SR, Turner CM, Elliott JI, McDaid J, Hewitt R, Smith J, Pickering MC, Whitehouse DL, Cook HT, Burnstock G, Pusey CD, Unwin RJ, Tam FW.** P2X7 deficiency attenuates renal injury in experimental glomerulonephritis. *J Am Soc Nephrol* 20: 1275–1281, 2009.
30. **Vonend O, Turner CM, Chan CM, Loesch A, Dell'Anna GC, Srai KS, Burnstock G, Unwin RJ.** Glomerular expression of the ATP-sensitive P2X receptor in diabetic and hypertensive rat models. *Kidney Int* 66: 157–166, 2004.
31. **Yasui N, Kajimoto K, Sumiya T, Okuda T, Iwai N.** The monocyte chemotactic protein-1 gene may contribute to hypertension in Dahl salt-sensitive rats. *Hypertens Res* 30: 185–193, 2007.
32. **Yip L, Woehrle T, Corriden R, Hirsh M, Chen Y, Inoue Y, Ferrari V, Insel PA, Junger WG.** Autocrine regulation of T-cell activation by ATP release and P2X7 receptors. *FASEB J* 23: 1685–1693, 2009.
33. **Yu T, Junger WG, Yuan C, Jin A, Zhao Y, Zheng X, Zeng Y, Liu J.** Shockwaves increase T-cell proliferation and IL-2 expression through ATP release, P2X7 receptors, and FAK activation. *Am J Physiol Cell Physiol* 298: C457–C464, 2010.

Biomedical Research 34 (6) 309-319, 2013

Renoprotective mechanisms of pirfenidone in hypertension-induced renal injury: through anti-fibrotic and anti-oxidative stress pathways

Xu Ji[1, 2], Yukiko Naito[2], Huachun Weng[2], Xiao Ma[2], Kosuke Endo[2], Naoko Kito[2], Nariaki Yanagawa[2], Yang Yu[1], Jie Li[1], and Naoharu Iwai[2]

[1] State Key Laboratory of Phytochemistry and Plant Resources in West China, Kunming Institute of Botany, Chinese Academy of Sciences, Kunming, Yunnan 650201, China and [2] Department of Genomic Medicine, National Cerebral and Cardiovascular Center, Suita 5658565, Japan

(Received 30 September 2013; and accepted 17 October 2013)

ABSTRACT

Pirfenidone (PFD) is a novel anti-fibrotic agent that targets TGFβ. However, the mechanisms underlying its renoprotective properties in hypertension-induced renal injury are poorly understood. We investigated the renoprotective properties of PFD and clarified its renoprotective mechanisms in a rat hypertension-induced renal injury model. Dahl salt-sensitive rats were fed a high-salt diet with or without 1% PFD for 6 weeks. During the administration period, we examined the effects of PFD on blood pressure and renal function. After the administration, the protein levels of renal TGFβ, Smad2/3, TNFα, MMP9, TIMP1, and catalase were examined. In addition, total serum antioxidant activity was measured. Compared to untreated rats, PFD treatment significantly attenuated blood pressure and proteinuria. Histological study showed that PFD treatment improved renal fibrosis. PFD may exert its anti-fibrotic effects via the downregulation of TGFβ-Smad2/3 signaling, improvement of MMP9/TIMP1 balance, and suppression of fibroblast proliferation. PFD treatment also increased catalase expression and total serum antioxidant activity. In contrast, PFD treatment did not affect the expression of TNFα protein, macrophage or T-cell infiltration, or plasma interleukin 1β levels. PFD prevents renal injury via its anti-fibrotic and anti-oxidative stress mechanisms. Clarifying the renoprotective mechanisms of PFD will help improve treatment for chronic renal diseases.

Pirfenidone (PFD; 5-methyl-1-phenylpyridin-2-one) is an anti-fibrotic agent. PFD has been considered as an antagonist of transforming growth factor β (TGFβ), and has anti-fibrotic, anti-inflammatory, and anti-oxidative stress activities (6, 12–14, 27, 36). PFD has demonstrated an anti-fibrotic effect via the down-regulation of TGFβ expression in several animal nephropathy models, including unilateral ureteral obstruction (36), diabetic nephropathy (24, 27), nephrectomy (35, 38), vanadate-induced renal fibrosis (1), and calcineurin inhibitor-induced nephrotoxicity (5, 6, 34). In addition, the clinical effectiveness of PFD has been evaluated in human diabetic nephropathy (32) and focal segmental glomerulosclerosis (7). The anti-fibrotic effect of PFD might also be due to the regulation of the balance of matrix metalloproteinases (MMPs) and their inhibitors, tissue inhibitors of metalloproteinases (TIMPs) (6, 10, 20, 36). Furthermore, PFD may also exert its anti-fibrotic effect via the suppression of fibroblast proliferation (14).

PFD has demonstrated anti-inflammatory effects via the inhibition of the expressions of inflammatory mediators such as tumor necrosis factor α (TNFα) and interleukin 1β (IL1β) both *in vivo* and *vitro* (2,

Address correspondence to: Xu Ji, PhD or Yukiko Naito, PhD
Department of Genomic Medicine, National Cerebral and Cardiovascular Center, 5-7-1 Fujishirodai, Suita, Osaka 565-8565, Japan
Tel: +81-6-6833-5012 (Ext 2513), Fax: +81-6-6835-2088
E-mail: jixu@mail.kib.ac.cn or naitoy@ncvc.go.jp

12, 13, 20). Oxidative stress is related to progressive renal injury (28). PFD is reported to exert antioxidative stress in mesangial cells and in a cirrhosis model (27, 30). Therefore, the anti-inflammatory and anti-oxidative stress effects of PFD are also expected to ameliorate renal injury. At present, although some renoprotective mechanisms of PFD have been reported, no systematic study has clarified the renoprotective mechanisms of PFD. Furthermore, the mechanisms underlying the renoprotective action of PFD in hypertension-induced renal injury are poorly understood. Therefore, the present systematic study investigated the anti-fibrotic, anti-inflammatory, and anti-oxidative stress effects of PFD. To elucidate the mechanisms underlying the renoprotective action of PFD, we administered PFD to Dahl salt-sensitive rats, and measured blood pressure and renal function. We also investigated the effects of PFD on TGFβ protein levels as well as its upstream and downstream signaling pathways. The PFD-induced protein expression changes of MMP9 and TIMP1 were examined. The effects of PFD on fibroblast proliferation were also investigated by immunohistochemistry. In addition, the effects of PFD on inflammatory factors such as macrophage and T-cell infiltration, TNFα protein expression, and plasma levels of IL1β were examined. Finally, we investigated catalase protein expression and total serum antioxidant activity.

MATERIALS AND METHODS

Experimental animals. Dahl salt-sensitive rats were obtained from SLC Japan (Shizuoka, Japan). The rats were housed in a temperature-controlled pathogen-free room with light from 0700 to 1900 h (daytime) and had free access to food and water. Experiments were performed in accordance with the guidelines of the National Institutes of Health Guide for the Care and Use of Laboratory Animals, and the experimental protocols were approved by the National Cerebral and Cardiovascular Center for the Care and Use of Experimental Animals.

Renoprotective effects of PFD in Dahl salt-sensitive rats. Dahl salt-sensitive rats were fed a high-salt diet [8% NaCl (w/w); Oriental Yeast, Tokyo, Japan] from 4.5 weeks of age. PFD-treated Dahl salt-sensitive rats (PFD group, n = 10) were fed the high-salt diet with mixed with 1% PFD (approximately 700 mg kg^{-1} day^{-1}). Control Dahl salt-sensitive rats (Control group, n = 10) were administered only the high-salt diet. Rats were treated with PFD for 6 weeks. PFD was provided by Shionogi (Osaka, Japan).

Blood pressure was measured once every 2 weeks using a tail-cuff method (BP-98A; Softron, Tokyo, Japan). Rats were housed in metabolic cages once every 2 weeks for 24-h urine collection. Urinary protein levels were measured using a BCA protein assay kit (Thermo Scientific, Rockford, IL, USA). Creatinine clearance (C_{Cr}) at week 6 of administration was calculated using the following formula: $C_{Cr} = (U_{Cr} \times V) / P_{Cr}$; U_{Cr} is the concentration of urinary creatinine (mg • mL^{-1}), P_{Cr} is the concentration of plasma creatinine (mg • mL^{-1}), and V is the urine flow rate (mL • min^{-1}). Creatinine levels were measured using a QuantiChrom creatinine assay kit (DIUR-500; BioAssay Systems, Hayward, CA, USA).

Measurement of TGFβ mRNA in the Dahl salt-sensitive rat kidneys. After 6 weeks with or without PFD treatment, the rats were anesthetized with pentobarbital (25 mg • kg^{-1}). Venous blood was collected from the vena cava. Plasma (EDTA as an anticoagulant) and serum were isolated by centrifugation and stored at −80°C until measurement. The left kidneys of the rats were removed, weighed, and sectioned longitudinally. Half of each left kidney was frozen in liquid nitrogen and stored at −80°C until measurement, while the other half was used to isolate RNA with TRIzol reagent (Invitrogen, Carlsbad, CA, USA) according to the manufacturer's instructions. TGFβ mRNA expression levels were determined by real-time RT-PCR using a commercial kit (Rn01442102_m1; Applied Biosystems, Foster City, CA, USA) and normalized to the expression of β-actin mRNA; these measurements were expressed as $\log_{10} (2^{35\text{-}CT1} / 2^{25\text{-}CT2})$, where $2^{35\text{-}CT1}$ and $2^{25\text{-}CT2}$ correspond to the expression levels of TGFβ and β-actin mRNA, respectively, as described previously (17).

Western blotting. Western blot analysis was performed using the extracts from rat kidneys frozen in liquid nitrogen and homogenized in 1% NP-40 lysis buffer as described previously (15). Equal amounts of protein (40 μg) were separated by SDS-PAGE (10% gels) and then transferred to a nitrocellulose membrane (Hybond ECL, 0.22 μm; GE Healthcare, Buckinghamshire, UK) or a PVDF membrane (Hybond-P, 0.45 μm; GE Healthcare). After blocking with 5% (w/v) skim milk powder, the membranes were incubated overnight at 4°C with primary antibodies (Santa Cruz Biotechnology, Santa Cruz, CA, USA) against TGFβ, Smad2/3, phosphorylated Smad2/3 (pSmad2/3), chromosome 3p kinase (3pK), homeodomain-interacting protein kinase 2 (HIPK2),

TNFα, MMP9, TIMP1, and catalase at 1 : 500 dilution. Membrane-bound antibodies were visualized with a horseradish peroxidase-conjugated secondary antibody (Amersham Biosciences, Buckinghamshire, UK) at 1 : 10000 dilution and an ECL advanced Western blotting detection kit (GE Healthcare). β-Actin (Santa Cruz Biotechnology) was used as a loading control.

Histological examination. As previously reported (16), for histological evaluation, the rats on week 6 of high-salt intake with or without PFD treatment were anesthetized with pentobarbital (25 mg • kg^{-1}) and portions of the right kidney were fixed in 10% buffered formalin-saline overnight at 4°C and subsequently embedded in paraffin blocks. Tissue sections 5-μm thick were stained with Masson's trichrome. The area of renal fibrosis was measured and analyzed with a BZ Image Analyzer II (Keyence, Osaka, Japan).

Immunohistochemistry. Immunohistochemistry was used to detect macrophages (CD68), T cells (CD3), and fibroblasts (FSP1, fibroblast-specific protein 1). After deparaffinization and antigen retrieval, endogenous peroxidase activity was blocked by 3.3% H_2O_2 and nonspecific binding was blocked by 5% normal goat serum. The sections were incubated overnight at 4°C with primary antibodies against CD68 (Abcam, Cambridge, UK), CD3 (BD Pharmingen, San Diego, CA, USA), and FSP1 (Abcam). The Simplestain MAX-PO (rat) kit (Nichirei, Tokyo, Japan) was used as a secondary antibody and allowed to incubate for 30 min at room temperature. Antibody binding was visualized using 3,3'-diaminobenzidine (DAB; Dojindo Laboratories, Kumamoto, Japan), and the nuclei were stained with hematoxylin. The numbers of positive cells were counted, and the results are expressed as the number of positive cells per square millimeter renal tissue.

Plasma IL1β measurement. Plasma IL1β was measured in duplicate with an enzyme-linked immunosorbent assay (ELISA) kit (IBL, Gunma, Japan).

Measurement of total serum antioxidant activity. To evaluate reactive oxygen species, we determined the total serum antioxidant activity by using the total antioxidant power colorimetric microplate assay kit (Oxford Biomedical Research, Oxford, MI, USA), which measures the reductive capacity by detecting the reduction of Cu^{2+} to Cu^{+}.

Statistical analysis. Values are expressed as mean ± standard error of the mean (SEM). Statistical analyses were performed using JMP (SAS Institute, Cary, NC, USA). Analysis of variance (ANOVA) was used to estimate differences among groups, and the significance of differences was tested using Student's *t*-test.

RESULTS

Effects of PFD treatment on body weight, urinary protein, C_{Cr}, heart rate, and blood pressure

Between the Control and PFD groups, there were no significant differences in body weight (Fig. 1A) and food intake (data not shown). Neither urine volume (Fig. 1B) nor water intake (data not shown) was significantly different between the Control and PFD groups. In contrast, urinary protein excretion was significantly attenuated at weeks 2 and 4 after the PFD treatment, indicating that PFD exerted a renoprotective effect (Fig. 1C). Although a trend demonstrating the improvement of C_{Cr} was observed after 6 weeks of PFD treatment (Fig. 1D), there was no significant difference between the Control and PFD groups (1.58 ± 0.22 vs. 2.93 ± 0.66 mL • min^{-1}, respectively; $P = 0.13$).

PFD treatment did not affect heart rate as measured by the tail-cuff method (Fig. 1E). Six weeks of 8% NaCl diet feeding increased systolic blood pressure (SBP) in the Control group significantly. PFD treatment significantly attenuated this increase in SBP at weeks 2 and 4 (Fig. 1F).

From the results described above, we conclude that PFD treatment ameliorates hypertension and renal injury.

Effects of PFD treatment on renal weight and fibrosis

There were no significant differences in renal weight between the Control and PFD groups at week 6 (Fig. 2A). Six weeks of 8% NaCl diet feeding caused tubular dilatation, interstitial fibrosis, and glomerular sclerosis (Fig. 2C); PFD treatment significantly attenuated these pathological changes (Fig. 2D). PFD treatment markedly reduced fibrotic areas (Fig. 2B).

Effects of PFD treatment on renal TGFβ, Smad2/3, pSmad2/3, 3pK, and HIPK2 expression

PFD exerts a renoprotective effect via the downregulation of TGFβ expression (1, 5–7, 24, 27, 34–36, 38). Therefore, we examined whether PFD regulates TGFβ expression in a rat salt-sensitive hypertension model. Indeed, PFD treatment significantly reduced the mRNA (Fig. 3A) and protein (Fig. 3B) expres-

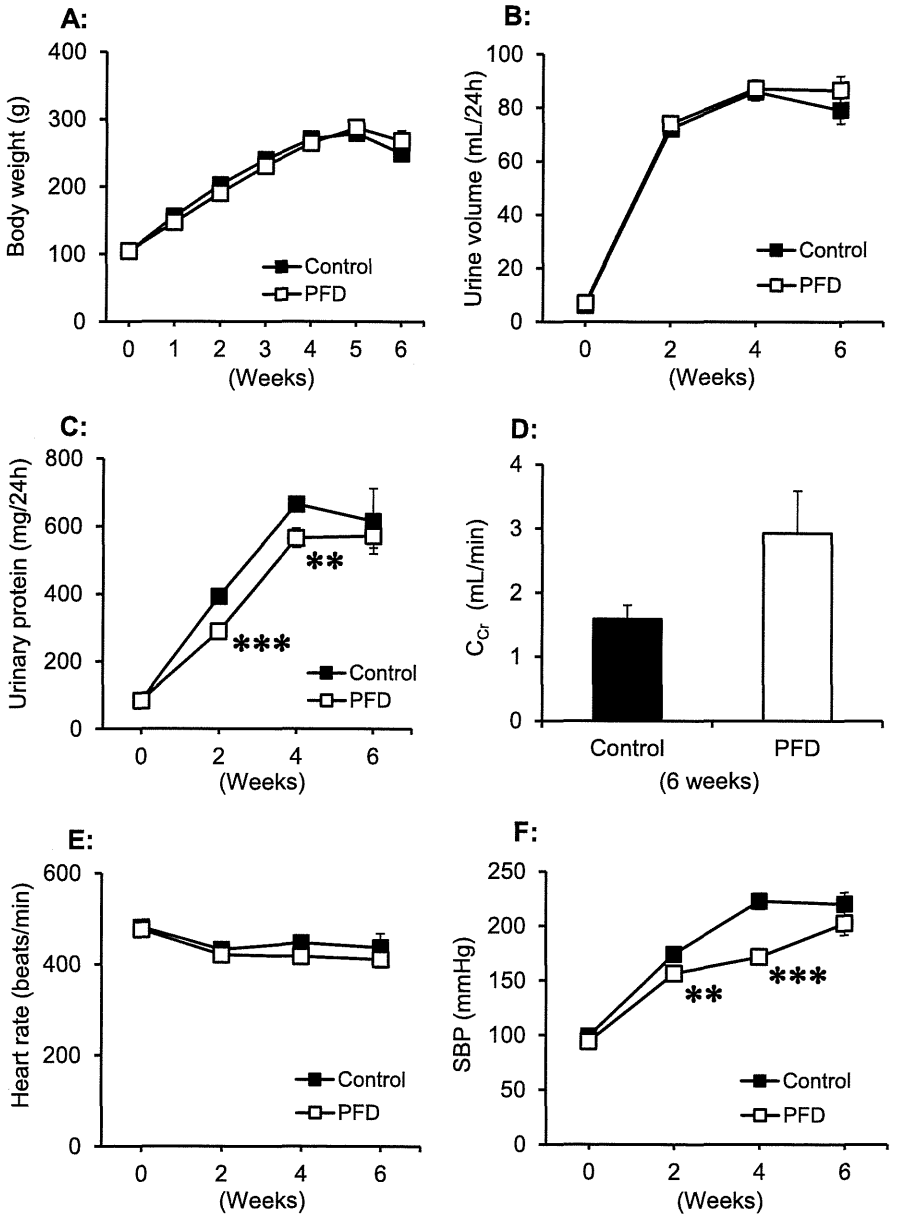

Fig. 1 Effects of PFD treatment on body weight, urinary protein, C_{Cr}, heart rate, and blood pressure. PFD-treated Dahl salt-sensitive rats (PFD group, n = 10) were fed a high-salt diet mixed with 1% PFD for 6 weeks. Control Dahl salt-sensitive rats (Control group, n = 10) were administered only the high-salt diet. Heart rate and SBP were measured by the tail-cuff method. There were no significant differences with respect to body weight (A), urine volume (B), C_{Cr} (D), or heart rate (E) between the Control and PFD groups. Six weeks of the 8% NaCl diet significantly increased urinary protein excretion (C) and SBP (F) in the Control group; PFD treatment significantly attenuated these increases in urinary protein excretion (C) and SBP (F) at weeks 2 and 4. $^{**}P < 0.01$, $^{***}P < 0.001$, significantly different from the Control group (unpaired Student's *t*-test).

sions of renal TGFβ compared to the Control group. TGFβ activates a unique signal transduction pathway that acts via the Smad family of proteins (9, 27). In the present study, PFD treatment did not affect the protein expression of total Smad2/3 (Fig. 3C). However, PFD treatment significantly attenuated pSmad2/3 protein expression in the kidneys (Fig. 3D). PFD treatment also attenuated the ratio of pSmad2/3 and total Smad2/3 (Control vs. PFD treatment, 1.40 ± 0.16 vs. 0.83 ± 0.11, respectively; $P = 0.002$). These results confirm that PFD treatment does not affect total Smad2/3 production but decreases Smad2/3 activity.

TGFβ also activates Smad-independent signaling